Macromolecular Research, Vol. 10, No. 4, pp 221-229 (2002)

Poly(ethylene terephthalate)(PET) Nanocomposites Filled with Fumed Silicas by Melt Compounding

Su-Chul Chung, Wan-Gyu Hahm, and Seung-Soon Im*

Department of Textile and Polymer Engineering, College of Engineering, Hanyang University, Haengdang-dong, Seungdong-ku, Seoul 133-791, Korea

Seong-Geun Oh

Department of Chemical Engineering, College of Engineering, Hanyang University, Haengdang-dong, Seungdong-ku, Seoul 133-791, Korea

Received June 8, 2002 ; Revised July 30, 2002

Abstract : PET nanocomposites filled with fumed silicas were prepared via direct melt compounding method at various mixing conditions such as filler type and filler content. Some fumed silicas were pre-treated to improve the wettability and dispersibility, and principal characterizations were performed to investigate the effects of nano fumed silicas on polymer matrix. Hydrophobic fumed silica (M-FS), which has the similar contact angles of water with neat PET, acted as the best reinforcement for the thermal stability and mechanical properties of PET nanocomposite, and FE-SEM images also showed that M-FS was uniformly dispersed into matrix and had good wettability. But, some filler (O-FS) had low dispersibility and caused the deterioration of mechanical properties. Besides, the results of DSC revealed the nucleation effect of all fillers in polymer matrix, and PET nanocomposite filled with hydrophilic fumed silica (FS) showed markedly the characteristic dynamic rheological properties such as shear thinning behavior at very low frequencies and the decrease of viscosity.

Keywords : poly(ethylene terephthalate), nanocomposite, fumed silica, melt compounding, rheology.

Introduction

Poly(ethylene terephthalate)(PET) is an excellent commercial thermoplastic polymer, which is in use for very wide scope such as textile/industrial yarn, film, injection mold and bottle, and the various fillers have been applied to solid additives incorporated into the PET polymer in order to modify its mechanical, thermal and chemical properties. Recently, the nano size fillers are attracting a great deal of attention,[1] because the properties of filled polymers can be taken much beyond their intrinsic values. But, some critical problems: the complicate and special conditions of filler modification, the low heat-resistance of modifier in high mixing temperature, and inferior processability due to the increase of viscosity still restrict the mass production and various application of the PET nanocomposite.

Nano fumed silica[2] has been used in industry as a rheological additives and the useful reinforcement of thermosetting polymer. Hydrophilic fumed silica can be chemically modified to hydrophobic fumed silica easily,[3] and has extremely large and smooth non-porous surfaces[2,4,5] promoting the strong physical contact between filler and polymer matrix. In addition, the particle-particle interactions of fumed silicas lead to the agglomerates and particle networks related to the shear thinning effect,[6,7] and H. Barthel ascertained that these interactions depend heavily on the difference of polarity between filler and liquid medium.[8] Thus, if the fumed silicas have similar hydrophobic/hydrophilic properties to polymer matrix, they would be more effectively dispersed and wetted with matrix, and It is expected that fumed silicas act as new suitable nano-reinforcement to improve the heat deflection temperature and the barrier to diffusion of solvent apart from increasing the modulus even at low filler content.[9]

Sumita *et al.*[10] reported that nano silica particles give rise to higher rigidities and yield stress in silica filled polyamide 6, and some research groups have studied the characteristics of the polymer-fumed silica nanocomposites based on polyamide 6,[11] polypropylene,[12] and polyurethane.[13] In the case of PET, some interesting results, for examples the delay of crystallization in undrawn pre-oriented polyester yarns at high speed spinning[14] and the improvement of uniformity of

*e-mail : imss007@hanyang.ac.kr

fully drawn multifilamentary PET yarn in high speed spinning,[15] were reported when the very small part of nano fumed silicas were added. But, there are barely systematic researches in various behaviors of PET nanocomposite filled with fumed silica.

Therefore, the aim of the present study is to investigate the effects of various nano fumed silica on thermoplastic PET polymer as a function of the filler content. PET nanocomposites were prepared by conventional direct melt compounding, which would be more economical and simple than in situ polymerization process and greatly expand the applicable opportunities. The characterizations of nanocomposites for instance thermal properties, dynamic rheological behaviors, mechanical performance, and morphological changes were investigated and discussed in detail.

Experimental

Materials. Polyethylene terephthalate(PET), Intrinsic Viscosity 0.655 dL/g and for fiber and film, was supplied by Toray-Saehan Co. Ltd. The hydrophilic neat fumed silica of primary particle size average 7 nm was purchased from Sigma and the surface modifiers, methyltrichlorosilane and octadecyltrichlorosilane were purchased from Aldrich. Toluene was obtained as ACS grade and used as solvent without further purification. More detailed properties of the materials used in this work are given in Table I.

Surface Modification of Fumed Silicas and Their Characterization. Hydrophobic surface modifications of neat fumed silica (FS) by methyltrichlorosilane (M-FS) and octadecyltrichlorosilane (O-FS) were treated through the following procedures[16]: The surface modifier of 10 wt% for the total mixture was first added to the toluene solvent by stirring. FS (7 nm) of 5 wt% for the total mixture was then added to the solution, and the final mixture was stirred for 6 h at room temperature. The homogeneous mixture, which finished the substitution, was kept in rotary evaporator to remove a majority of the solvent and then the dregs of the solvent was eliminated in vacuum oven at 90 °C for 24 h. The cohesion matters of silicas were pulverized with a mortar, and the final surface modified silica particles were dried in vacuum oven at 90 °C for 24 h again.

In order to verify the surface modification of fumed silica, Fourier transform infrared (FT-IR) was carried out using Nicol 760 MAGNA-IR spectrometer. The methanol wettability was calculated as remarked in Table II,[17] and the contact angles for pressed silica pellets were measured with distilled water using G-type ERMA Inc.

Figure 1 shows the FT-IR spectra for fumed silicas. New (a) strong stretching bands at 2975~2840 cm^{-1} and (b) bending bands at 1480~1440 cm^{-1} of methylene groups in octadecyl chains appear in O-FS spectrum, and the symmetric deformation peak of methyl group, which bonded to silicon atoms, also appear at (c) 1280~1250 cm^{-1} in M-FS spectrum. Especially, the broad absorption peak at 3700~3200 cm^{-1} due to Silanol Group (Si-OH) definitely decreases in the case of M-FS and O-FS. Besides, the more weight loss of *M-FS and O-FS against FS in TGA tests (Table III) could* be also explained in terms of the thermal degradation of alkyl groups on these silica surfaces. These results therefore indicate that the surface modifications of fumed silicas were suitably performed.

The data of methanol wettability and contact angles in Table II reveal the degree of hydrophobic/hydrophilic property for each silicas. As expected, O-FS and M-FS have hydrophobic property, but FS has completely hydrophilic property. The reason O-FS has more strong hydrophobic property than M-FS would be assumed that the chemical reactivity of octadecyltrichlorosilane with silanol groups is much superior to that of methyltrichlorosilane, or O-FS has long octadecyl chains, which can cover and interrupt some un-reacted silanol groups on the surface of the silica.

Preparation of PET Nanocomposites and Their Char-

Table II. The Degree of Hydrophobic for Each Fillers

Filler	Methanol Wettability(%)[a]	Contact Angle (deg.)[b]
FS	0	-
M-FS	11.5	57
O-FS	53.2	113

[a]Methanol wettability(%) = $(a \times 0.79)/(a \times 0.79 + 50)100$; *a*: Total volume(mL) of added methanol until the filler of 0.2 g was completely precipitated in distilled water of 50 mL.
[b]Measured with distilled water (contact angle of PET: 79.09± 0.12deg.).

Table I. The Materials Used in This Study

Materials	Supplier(Product No.)	Typical Properties
Poly(ethylene terephthalate) (PET)	TORAY SAEHAN (SBR A-9203)	IV: 0.655± 0.008; Haze: < 1%; D-EG: 1.0± 0.2%; COOH: 34± 6; TiO_2: 0%; Used for film and fiber
Fumed silica	Sigma	Blue-gray powder; Primary particle size: 7 nm; Surface area: 390± 40 m^2/g; Purity grade: > 99.8%; Hydroxyl groups: 3.5~4.5/nm^2
Methyltrichlorosilane (CH_3SiCl_3)	Aldrich	Colorless liquid; MW: 149.48; Density: 1.273g/cm^2; Assay: 97%; b_p760: 66 °C
Octadecyltrichlorosilane ($CH_3(CH_2)_{17}SiCl_3$)	Aldrich	Colorless liquid; MW: 387.94; Density: 0.984g/cm^2; Assay: 90+%; b_p10: 223 °C

acterization. PET nanocomposites were prepared via direct melt compounding method using Haake twin roll counter-rotating mixer at various mixing conditions such as filler type (FS, M-FS, and O-FS) and filler content (0.5~8.0 wt%). Besides, the total mixing weight of materials per batch was 50 g and the compounding was carried out under a barrel temperature of 280 °C, roll speed of 60 rpm, and mixing time of 5 min in consideration of polymer degradation due to shear heating. All materials had been dried in vacuum dryer at 90 °C for 24 h before used.

Thermal properties of nanocomposites were analyzed in a nitrogen atmosphere by differential scanning calorimetry (Perkin-Elmer DSC 7). To remove previous thermal history, all samples were first heated at 270 °C for 3 min and then quenched to 30 °C at a rate 500 °C/min. The second scanning of heating and cooling was then performed at a rate 10 °C/min. The thermogravimetric analysis (TGA) was also performed under air purge at a heating rate of 10 °C/min in the same instrument. The isothermal crystallization behavior of the composite was observed using a polarization microscope (Nikon HFX-11A) at crystallization temp. of 230 °C for 1 h in the isothermal instrument (METTLER TOLEDO).[18]

Mechanical properties were measured at room temperature by the tensile testing machine (Instron-4465, Instron Corp.) according to ASTM D882 method, and all samples were prepared with film using hot press (CARVER, model 2699) at 280 °C for 3 min and then quenched in chilled water of 15 °C. The morphology of the fractured surface for each sample after tensile test and the alkali treated surface were observed using a Field Emission Scanning Electron Microscope (FE-SEM, JEOL, JSM-6330F), and all samples for SEM were coated with Pt for 5 min. The alkali treatment for the surface of PET nanocomposites was performed under NaOH solution of 10 o.w.f% at 80 °C for 12 h.

The rheological behaviors at the melt state for nanocomposite systems were examined by the dynamic oscillatory viscometer (ARES, Rheometric Scientific Inc.) using a parallel-plate geometry that has a diameter of 20 mm and gap of 1.0 mm. This experiment was performed at melting temp. of 270 °C, the strain level of 10%, and the frequency swept from 0.1 to 400 rad/s.

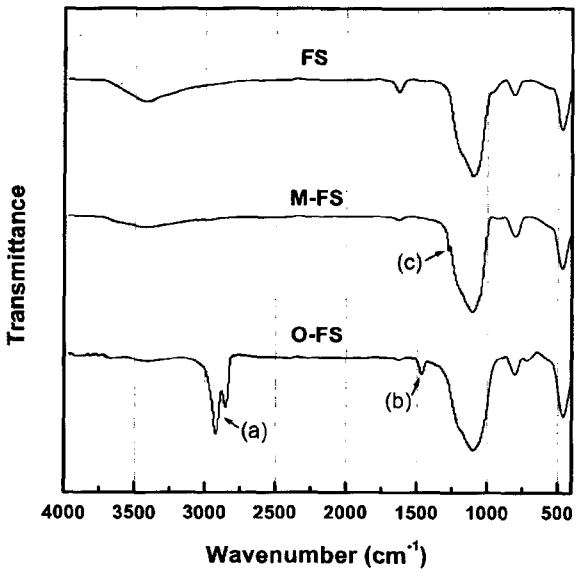

Figure 1. FT-IR spectra of different fumed silicas: FS, M-FS and O-FS.

Table III. Thermogravimetry Data of PET and Its Nanocomposites

Samples	T_D^i(°C)[a]	T_D^5(°C)[b]	$wt._R^{700}$(%)[c]
PET	335	364	0.1
PET/FS(8 wt.%)	357	392	7.6
PET/M-FS(8 wt.%)	383	402	7.5
PET/O-FS(8 wt.%)	334	390	3.9

[a,b]The temperature at weight reduction of 2 and 5%.
[c]The weight percent of residue at 700 °C.

Results and Discussion

Thermal Properties and Crystallization Behavior of PET Nanocomposites. A typical thermogravimetric curves are presented in Figure 2 and the results of TGA are summarized in Table III. As shown in Figure 2, the neat PET starts to decompose at about 300 °C and weight loss increases rapidly, whereas PET/FS and PET/M-FS are stable up to higher temperature and draw the similar slop of weight loss curves. PET/O-FS shows a small weight loss from about 260 °C due to the decomposition of long octadecyl chains on the surface of O-FS. The initial thermal degradation temperature (T_D^i) of 2% in Table III reveals a maximum increase of 48 °C when PET filled with M-FS, and all PET nanocomposites are held higher temperature than neat PET over all

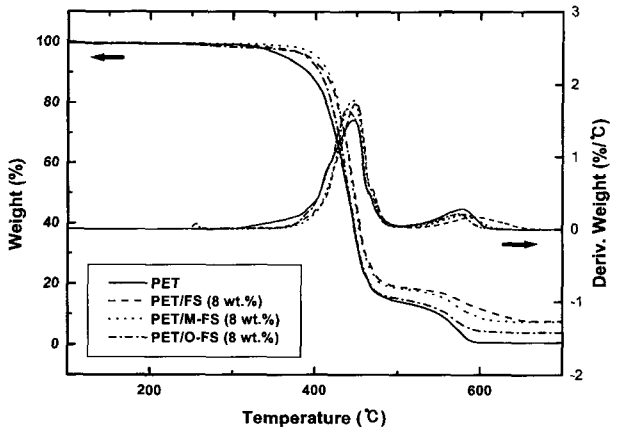

Figure 2. TGA variation of nanocomposites.

Table IV. DSC Data of PET and Its Nanocomposites

Samples	Actual Filler Content [ ][g] (wt%)		T_g[a] (°C)	T_c[b] Peak(°C)	T_c[b] ΔH_c(J/g)	T_m[c] Peak(°C)	T_m[c] ΔH_f(J/g)	T_c[d] Peak(°C)	ΔT[e] (°C)	X_c[f] (%)
PET			78.2	142.0	-30.0	255.0	46.3	198.0	57.1	13.0
PET/FS	0.5		77.4	136.5	-22.5	255.0	49.1	207.2	47.9	21.2
	2		76.8	130.5	-9.5	255.5	49.2	210.2	45.3	31.7
	8			121.7	-2.1	255.2	44.8	210.9	44.3	34.0
PET/M-FS	0.5	[0.49]	78.1	135.9	-20.9	255.0	47.2	204.5	50.5	21.0
	2	[1.95]	76.9	128.4	-7.8	254.9	45.6	206.1	48.8	30.1
	8	[7.82]		124.4	-1.5	254.9	43.3	209.6	45.3	33.3
PET/O-FS	0.5	[0.26]	78.3	140.2	-27.0	255.0	47.1	202.9	52.1	16.0
	2	[1.03]	77.2	139.2	-26.2	254.4	47.8	202.4	52.0	17.2
	8	[4.25]		126.5	-2.8	255.5	45.4	211.0	44.5	33.9

[a]The glass transition temperature measured on the second heating at 10.0 °C/min using half Cp Extrapolated method.
[b]The crystallization temperature measured on the second heating at 10.0 °C/min.
[c]The melting temperature measured on the second heating at 10.0 °C/min.
[d]The crystallization temperature measured on the second cooling at 10.0 °C/min.
[e]The degree of supercooling: (T_m^c peak - T_c^d peak).
[f]Apparent crystallinity: $(\Delta H_f - |\Delta H_c|)/\Delta H_f^0 \times 100$, ΔH_f^0: 125.5 J/g.
[g]Actual silica content determined by TGA at 800 °C.

range of weight loss. The residual weights at 700 °C increase with loading fumed silica and follow similarly actual filler contents in Table IV. The thermal stability of PET is therefore improved markedly by the addition of fumed silica, and the reason M-FS performs as the best thermal reinforcement would appear to be related to the good wettability and dispersitibility on the matrix.

DSC results in Table IV show the characteristic non-isothermal crystallization behaviors of PET nanocomposites against neat PET. Firstly, the melting peaks (T_m) and heat of fusion (ΔH_f) of all nanocomposites at the second heating are almost same as neat PET regardless of the filler type or filler content. But, the degree of super cooling (ΔT) decrease with increasing filler content in all nanocomposites, indicating that fumed silicas act as nucleating agents in polymer matrix and accelerate the crystallization rate.[13] The increase of the apparent crystallinity (X_c) with filler content also appears to result from the incidence of very rapid crystallization due to the nucleating effect of nano fillers, although all samples were quenched within the maximum limit of DSC before the second heating. Figure 3 shows the relation of apparent crystallinity and actual silica content for each nanocomposites in detail. The crystallinity of all nanocomposites increases rapidly until actual filler content of 2 wt%, but over this point it becomes to increase very slowly. Thus, these mean that the crystallization rate and crystallinity of all nanocomposites are only proportional to the actual filler content regardless of filler type and there are critical filler content as nucleating agents.

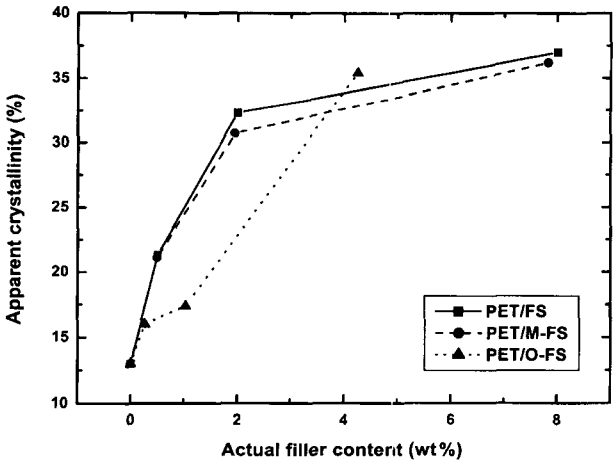

Figure 3. Variation of apparent crystallinity as a function of actual filler content for nanocomposites.

The effects of nano fillers on the isothermal crystallization for each nanocomposites are shown well in Figure 4. The neat PET has uniform and big spherulites, but the all nanocomposites have many small and irregular spherulites. It would prove once more that the silicas act as nucleating

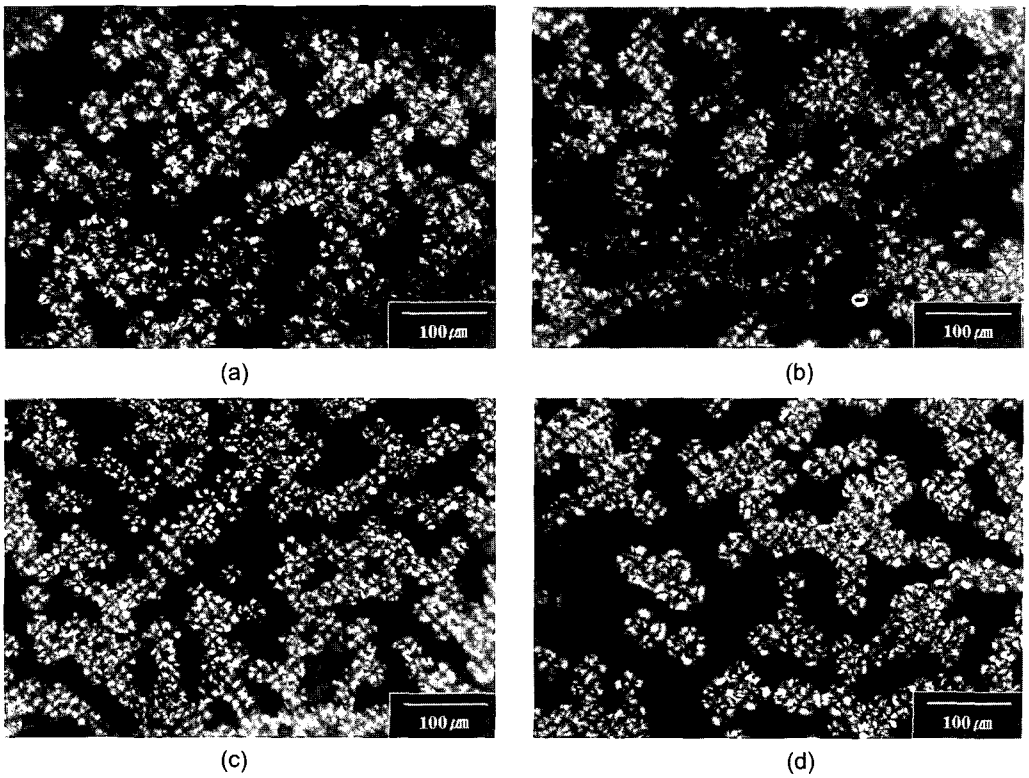

Figure 4. Spherulite photographs of isothermal crystallization of (a) neat PET, (b) PET/FS, (c) PET/M-FS, and (d) PET/O-FS (filler content of 2 wt%).

agents, increasing the number of spherulites. Especially, it is interesting that some growth patterns of spherulites in the form of line like some network structures are observed in PET/FS nanocomposites (Figure 4b).

Mechanical Properties and Morphology of PET Nanocomposites. Mechanical properties for PET nanocomposites filled with various surface-treated silicas as a function of filler content were shown in Figure 5. The tensile strength (Figure 5a) of PET/M-FS more increases than that of PET/FS until the filler content reaches 4.0 wt%, but the excessive filler loading induces the deterioration of the tensile strength and PET/O-FS monotonously decrease from low filler content. The elongation at break (Figure 5b) for the nanocomposites show also PET/M-FS is higher than others at the range of filler content of 1~4 wt%, although decreasing as filler content increase, but PET/FS and PET/O-FS decrease more rapidly even at low filler content.

Nielson Equation (1),[19,20] which is one of the most generalized theoretical equations to calculate the modulus (M) of a composite, presents well the relations of modulus and various factors.

$$\frac{M}{M_1} = \frac{1+(k_E-1)B\phi_2}{1-B\psi\phi_2} \quad (1)$$

where M_1 is any modulus of unfilled polymer, ϕ_2 is filler volume fraction, k_E is Einstein coefficient of filler and B is 1.0 for very large filler/matrix modulus ratio. The factor ψ depends on the maximum packing fraction ϕ_m of the filler, and McGee *et al.*[21] proposed following complex equation (2) when B is 1.0 and Einstein coefficient k_E is much greater than 1.0.

$$\psi = 1+\frac{\phi_1}{\phi_m}[\phi_m\phi_2+(1-\phi_m)\phi_1] \quad (2)$$

Besides, Lewis and Nielson[22] reported the maximum packing fraction ϕ_m and Einstein coefficient k_E are 0.37 and 6.76 for large agglomerates with spherical particles in random packing.

But, Figure 5c reveals that the actual moduli of PET/M-FS and PET/FS nanocomposites are higher than the conventional theoretical modulus (curve-A) calculated with the above conditions. According to Nielsen and Landels study, [9] this discrepancy could be explained as follows. The first reason is that the absorbed polymer layer at the interface give rise to the increase of volume fraction ϕ_2 or/and the values of M_1, because the surface area of the particles increases as the particle size decreases. But, it is more or less insufficient to understand the increase of the modulus only by this reason, and Reynaud *et al.*[11] also indicated there are no morphological manifestations for interphase layer. However, another suitable reason would be the additional decrease of maximum

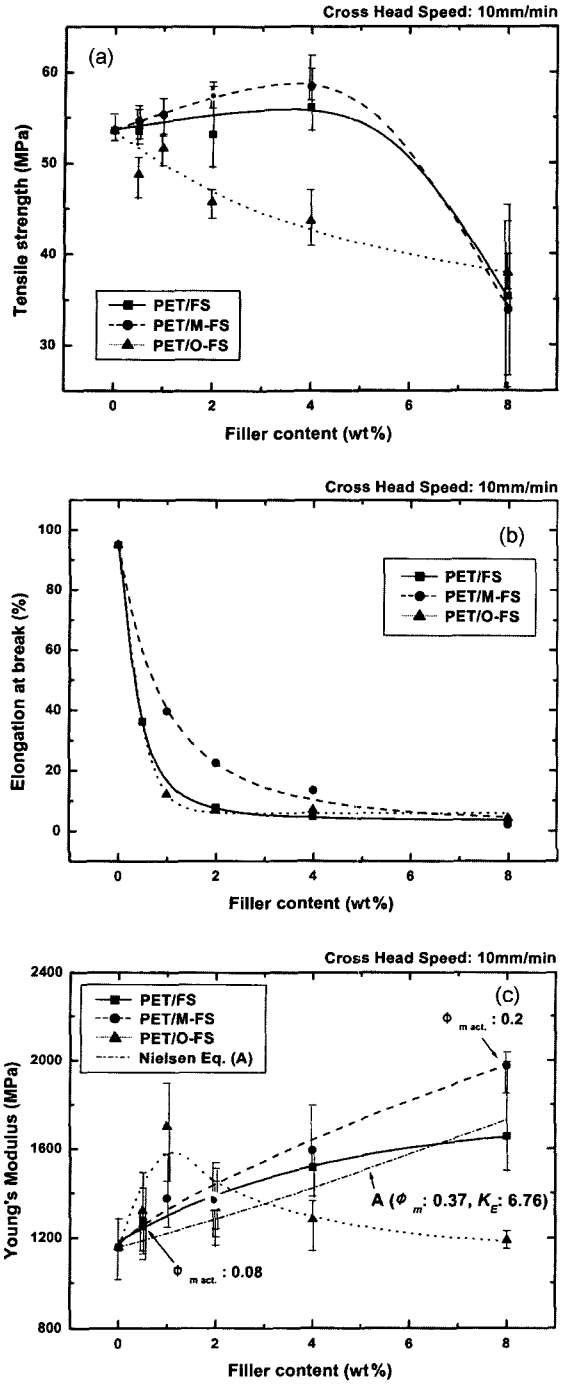

Figure 5. Variation of (a) tensile strength, (b) elongation at break, and (c) youngs modulus as function of filler content for nanocomposites.

packing fraction ϕ_m due to the agglomerates and strong network structure of fine nano-particles, and for examples if the actual maximum packing fractions $\phi_{m\ act}$ of M-FS in PET/M-FS are ranging from 0.08 to 0.2, the theoretical modulus corresponds to the actual modulus. The reason the modulus of PET/M-FS is higher than those of PET/FS and PET/O-FS would suggest that M-FS has the better contact with PET polymer matrix, or the actual maximum packing fractions $\phi_{m\ act}$ of FS and O-FS, which have lower dispersibility, is higher than that of M-FS due to the increase of packing effect.[23-26]

In order to prove the results of mechanical properties and to investigate certainly the dispersibility of fumed silicas in PET matrix, the method of alkali treatment with NaOH solution was performed. Nano fumed silicas were removed effectively with matrix from the surface of PET nanocomposites, and the morphology of various nano-size pores could be observed by SEM images. As expected, Figure 6 shows that pore sizes of PET/M-FS are smaller than those of PET/FS overall. But, PET/O-FS has big size filler aggregate remained in the matrix, although some small O-FS particles below 50 nm are shown also on the surface. These results reveal that the dispersibility of fumed silica in non-polar polymer matrix can be improved by hydrophobic surface treatment, but the surface modified silica with long alkyl chain (O-FS) tends to form firm aggregate, which can not be dispersed even by high shear force during melt compounding. In addition, it has been reported that the contact angle of water on the surface of neat PET was 79.09± 0.12 deg.[27] Since the contact angles of water on the surface of M-FS and O-FS are 57 and 113 deg. as shown in Table II, it might be inferred that the compatibility or wettability between M-FS and PET is better than that between O-FS and PET. Thus, O-FS has the lower despersibility in PET than M-FS, but the high modulus of PET/O-FS at low filler content in Figure 5c indicate that if O-FS has also good dispersibility and little agglomerates, O-FS can increase dramatically the modulus of composite, because O-FS has long alkyl chains on the surface, which can be physically entangled with matrix polymeric chain.

The SEM photomicrographs (Figure 7) for the fractured surfaces of specimens reveal the affinity of each filler for polymer matrix. As compared with PET/FS, fractured surface of PET/M-FS has a lot of elongated small deformations of polymer matrix, which would be the result of good wettability between M-FS and PET matrix. But, PET/O-FS shows also the broken aggregates of O-FS by the local deformation of polymer matrix, which causes the deterioration of mechanical properties.

Rheological Properties of PET Nanocomposites. The loss tangent (tan δ) for neat PET and its nanocomposites at melt state are shown in Figure 8. All nanocomposites at filler content of 2 wt% have lower tan δ and more elastic properties than neat PET at low frequency range, and the tan values of PET/FS and PET/M-FS are more remarkably decreased with increasing filler content over the frequency range (Figure 8b). The Cole-Cole plots in Figure 9 show also that all nanocomposites of 2 wt% (Figure 9a) draw similar curves and have low slope of about 0.89 at a low loss modulus (G'') value, indicating that the system is heteroge-

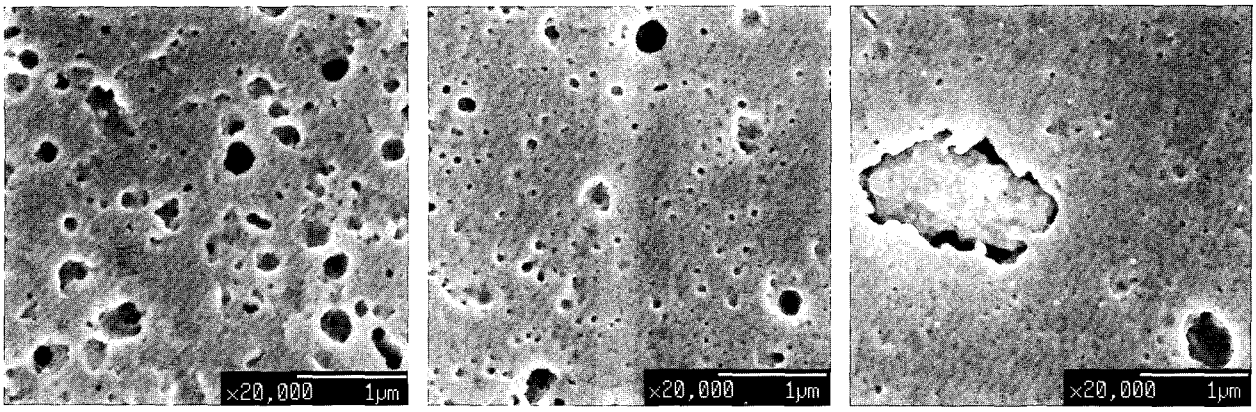

Figure 6. SEM photomicrographs of film surface of (a) PET/FS, (b) PET/M-FS, and (c) PET/O-FS (filler content of 4 wt%).

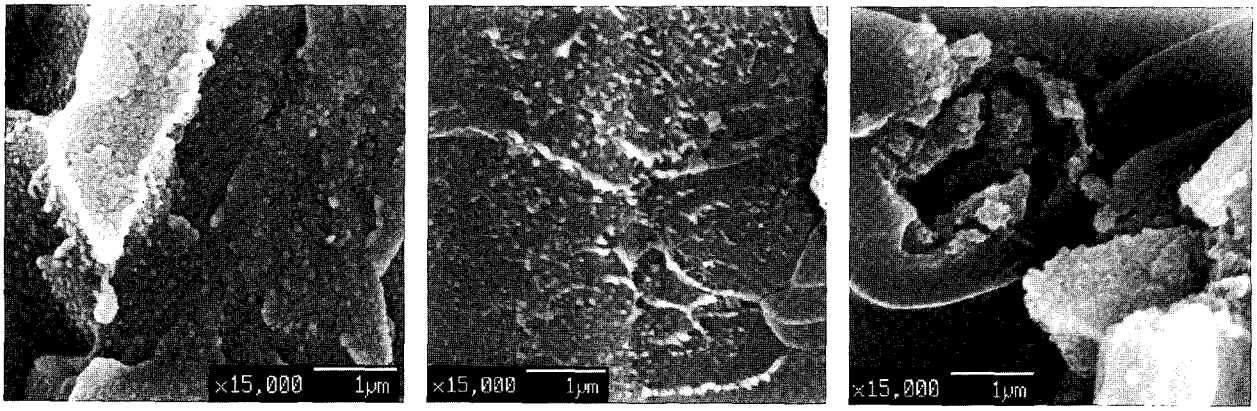

Figure 7. SEM photomicrographs of Instron fractured surface of (a) PET/FS, (b) PET/M-FS, and (c) PET/O-FS (filler content of 4 wt%).

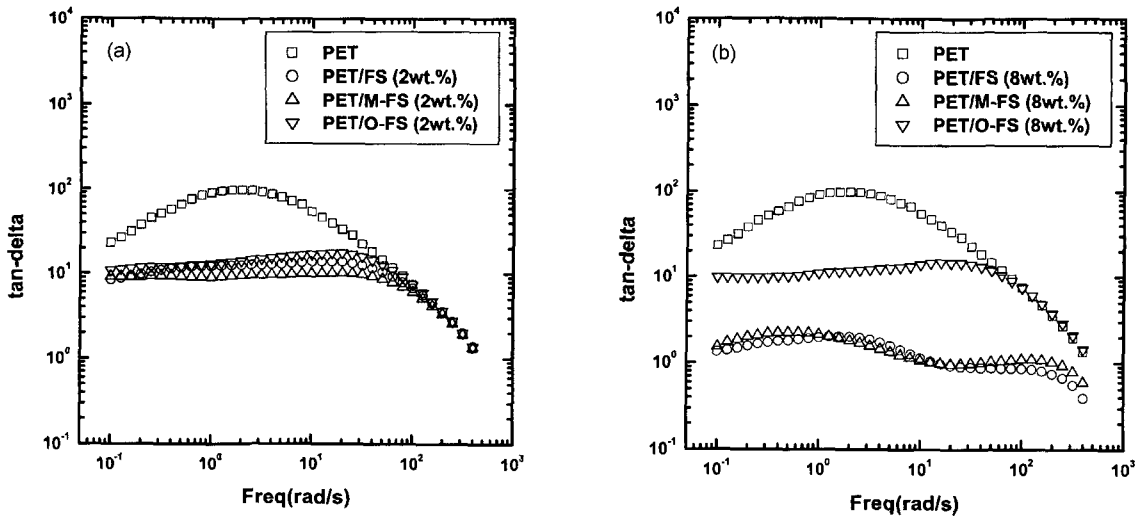

Figure 8. The loss tangent (tan δ) (a) at filler content of 2 wt%, and (b) at filler content of 8 wt% as function of frequency for nanocomposites (Temperature: 270 °C).

neity and much energy would be dissipated. But, over the loss modulus (G'') of about 10^3, the slopes of curves for nanocomposites increase and approach to neat PET curve whose slope is about 2.0. Thus, these reflect that there are some network structures due to filler interaction, collapsed by shear force, and after all interaction have collapsed the melt state becomes isotropic and homogeneous.[28] Especially, the Cole-Cole plot at filler content of 8 wt% in Figure 9b shows certainly the presence of filler interaction. The curves change more abnormally as the hydrophilic property of filler increases, and PET/FS shows the most solidlike elastic properties and the initial inflection point at the highest loss modulus (G'') of about 10^3 because of the strong network structures induced by hydrogen bonding of silanol group. The reason PET/M-FS follows similar pattern with PET/FS is assumed that considerable silanol groups, which could not react with modifier during the surface treatment, also remain on the surface of M-FS. The most hydrophobic PET/O-FS has no any particular change of curve with filler content.

The viscosity curve of nanocomposites in Figure 10 presents also interesting results, which denote the decrease of viscosity with filler addition. All nanocomposites at filler content of 2 wt% show that their shapes of viscosity curves are similar to neat PET but the viscosity values are slightly lower than that over the frequency range. In the case of high filler content of 8 wt%, although the viscosity of PET/FS and PET/M-FS show shear thinning behavior due to the breakdown of network structure even from a low frequency, PET/O-FS reveals same result correspond to the curve at low filler content of 2 wt% regardless of the variation of

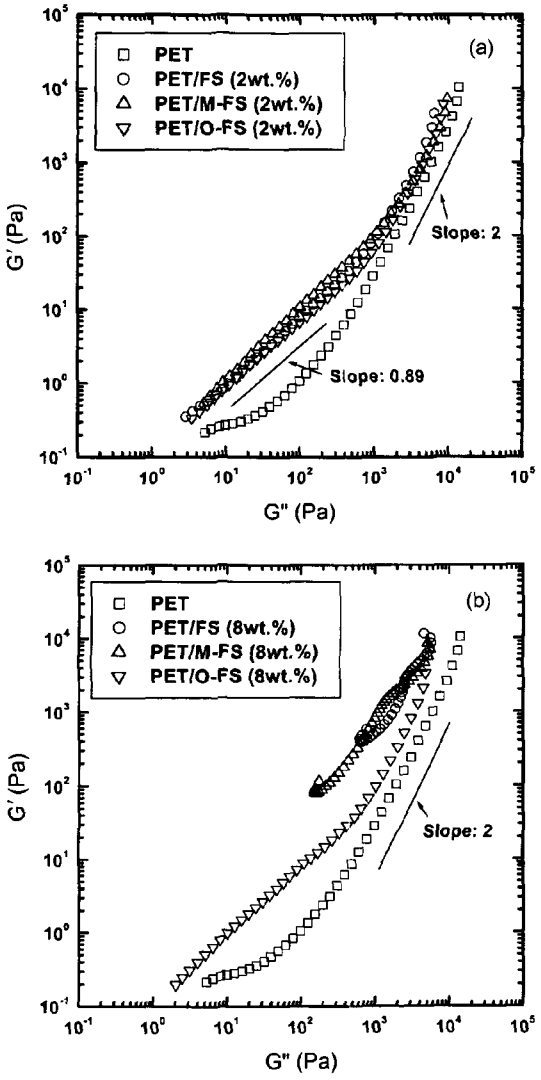

Figure 9. Cole-Cole plots (a) at filler content of 2 wt%, and (b) at filler content of 8 wt% for nanocomposites (Temperature: 270 °C; Frequency range: 0.1~400 rad/s).

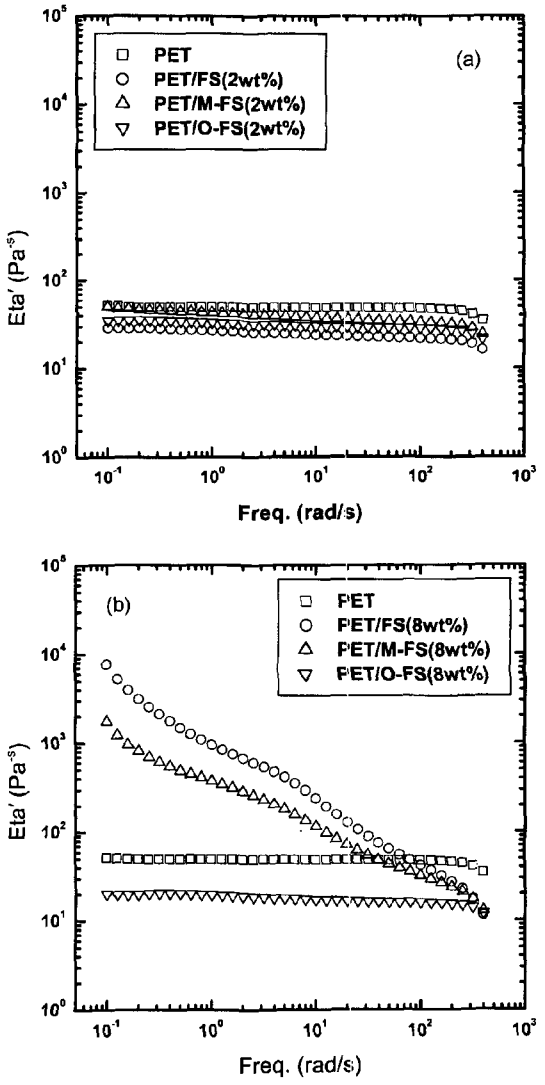

Figure 10. The melting viscosity (a) at filler content of 2 wt%, and (b) at filler content of 8 wt% as function of frequency for nanocomposites (Temperature: 270 °C).

frequency. Cho *et al.*[29] reported also about the reduction of melt viscosity for the nylon 6 nanocomposite filled with organoclay measured by capillary rheometry, and they suggested the some possible reasons: one is the slip between polymer matrix and filer, and another is the degradation of polymer matrix due to high shear heating during melt compounding. However, in this study it would indicate that the nano fumed silica act as lubricant at melting state of non-polar polymer, since fumed silica is consist of the spherical primary particles, which have smooth non-porous surface, of very low friction coefficient, but further study will be performed to explain more clearly this behavior.

Conclusions

Thermoplastic PET nanocomposites filled with various surface-treated fumed silicas were prepared via direct melt compounding as a function of filler content. The results of various characterizations showed that the thermal stability and mechanical properties of PET nanocomposites can be improved even at low filler content as increasing of the wettability and dispersibility of filler in the polymer matrix, and It was revealed that hydrophobic fumed silica (M-FS) is effective reinforcement for PET nanocomposite. Besides, all fumed silicas acted as nuclear agent and accelerated the crystallization rate of polymer.

The reason actual moduli of PET/M-FS and PET/FS nanocomposites are higher than the conventional theoretical modulus would suggest that fine nano fillers affect more the absorbed polymer layer at the interface and the maximum packing fraction ϕ_m. The Cole-Cole plot and loss tangent (tan δ) of dynamic rheological measurements presented that there are strong filler interaction and network structure induced by hydrogen bonding of silanol group in the melting composites and PET/FS has the most solidlike elastic properties. Especially, the decrease of melting viscosity of nanocomposites filled with fumed silicas can propose the possibility for the improvement of processability and various applications of the polymer nanocomposites.

Acknowledgements. This work was supported by the Next-generation new technology development project (#A18-05-07) of MOCIE. The authors, also, would like to thank TORAY SAEHAN INC for providing the PET chip.

References

(1) M.B. Ko, M. Park, J. Kim, and C.R. Choe, *Kor. Polym. J.*, **8(2)**, 95-101 (2000).
(2) *Technical Bulletin no. 6, no. 11*, Degussa Corporation, Aklon, OH, 1989.
(3) J. B. Donnet, M. J. Wang, E Papirer, and A. Vidal, *Kautsch, Gummi, Kunstst.*, **39(6)**, 510 (1986).
(4) H. Barthel, F. Achenbach, and H. Maginot, *Proc. Int. Symp. on Mineral and Organic Functional Fillers in Polymers (MOFFIS 93)*, Universite de Namur, Belgium, 301 (1993).
(5) A. J. Hurd, D. W. Schaefer, and J. E. Martin, *Phys. Rev. A*, **35(5)**, 2361 (1987).
(6) F. W. A. M. Schreuder and H. N. Stein, *Rheol. Acta*, **26**, 45 (1987).
(7) G. Lee, S. Murray, and H. Rupprecht, *J. Colloid Interf. Sci.*, **105(1)**, 257 (1985).
(8) H. Barthel, *Colloids and Surfaces A: Physicochemical and Engineering Aspects*, **101**, 217 (1995).
(9) L. E.Nielsen and R. F. Landel, *Mechanical Properties of Polymers and Composites*, Marcel Dekker, New York, 1994.
(10) M. Sumita, T. Shizuma, K. Miyasaka, and K. Ishikawa, *J. Macromol Sci. Phys.*, **B22(4)**, 601 (1983).
(11) E. Reynaud, T. Jouen, C. Gauthier, G. Vigier, and J. Varlet, *Polymer*, **42**, 8759 (2001).
(12) Min Zhi Rong, Ming Qiu Zhang, Yong Xiang Zheng, Han Min Zeng, R. Walter, and K. Friendrich, *Polymer*, **42**, 167 (2001).
(13) Ana M. Torro-Palau, Juan C. Fernandez-Garcia, A. Cesar Orgiles-Barcelo, and Jose Migual Martin-Martinez, *Int. J. of Adhes. and Adhes.*, **21**, 1 (2001).
(14) Antikow Paul and Pinaud Francois, United States Patent No. 5336709 (1994).
(15) James J. Breuning, Robert D. Johnson, and Gregory K. Morris, United States Patent No. 531976 (1984).
(16) S.Y. Oh, I.N. Kim, J.W. Choi, M.S. Kim, and H.D. Jang, *J. Korean Ind Eng. Chem.*, **11(9)**, 890 (2000).
(17) Heinz-Gunter Lux, Karl Meier, Astrid Muller, Rolf Oelmuller, and Anja Ramb, United States Patent No. 6.191.122 B1 (2001).
(18) J.K. Lee, K.H. Lee, and B.S. Jin, *Macromol. Res.*, **10(1)**, 44 (2002).
(19) T. B. Lewis and L. E. Nielsen, *J. Appl. Polym. Sci.*, **14**, 1449 (1970).
(20) L. E. Nielsen, *J. Appl. Phys.*, **41**, 4626 (1970).
(21) S. McGee and R. L. McCullough, *Polym. Comp.*, **2**, 149 (1981).
(22) T. B. Lewis and L. E. Nielsen, *Trans. Soc. Rheol.*, **12**, 421 (1968).
(23) J. G. Brodnyan, *Trans. Soc. Rheol.*, **12**, 357 (1968).
(24) H. S. Katz and J. V. Milewski, *Handbook of Fillers and Reinforcements for Plastics*, Van Nostrand Reinhold, New York, 1978.
(25) M. Al-Jarallah and E. Trons, *J. Test. Eval.*, **9**, 3 (1981).
(26) R. K. Gupta and S. G. Seshadri, *J. Rheol.*, **30**, 503 (1986).
(27) D. Li and A. W. Neumann, *J. of Colloid and Interf. Sci.*, **148**, 190 (1992).
(28) C. D. Han, J. Kim, and J. K. Kim, *Macromolecules*, **22**, 383 (1989).
(29) J. W. Cho and D. R. Paul, *Polymer*, **42**, 1083 (2001).